

Electron localization : band-by-band decomposition, and application to oxides.

M. Veithen,¹ X. Gonze,² and Ph. Ghosez¹

¹*Département de Physique, Université de Liège, B-5, B-4000 Sart-Tilman, Belgium*

²*Unité de Physico-Chimie et de Physique des Matériaux (PCPM),
place Croix du Sud, 1, B-1348 Louvain-la-Neuve, Belgium*

(Dated: November 8, 2018)

Abstract

Using a plane wave pseudopotential approach to density functional theory we investigate the electron localization length in various oxides. For this purpose, we first set up a theory of the band-by-band decomposition of this quantity, more complex than the decomposition of the spontaneous polarization (a related concept), because of the interband coupling. We show its interpretation in terms of Wannier functions and clarify the effect of the pseudopotential approximation. We treat the case of different oxides: BaO, α -PbO, BaTiO₃ and PbTiO₃. We also investigate the variation of the localization tensor during the ferroelectric phase transitions of BaTiO₃ as well as its relationship with the Born effective charges.

PACS numbers:

I. INTRODUCTION

In the study of periodic crystalline solids, the electronic ground-state wave function is usually described in terms of Bloch functions, delocalized on the whole system. As a consequence, for a long time, the understanding of electron localization in crystalline solids was mainly based on approximate pictures. Nevertheless, the basics of a quantitative characterization of electron localization had already been formulated by W. Kohn¹ in 1964. Recently this problematic was renewed, thanks to the development of the theory of polarization based on Berry phases^{2,3,4,5}, and the rigorous definition of the position operator in periodic systems^{6,7,8,9}. These ideas have been further developed using a cumulant generating function approach¹⁰.

Following these advances, Sgariello and co-workers¹¹, have computed the localization lengths for different cubic semiconductors, in the framework of the Kohn-Sham density functional theory^{12,13} (DFT). They showed that the degree of electron localization is quite different for the various investigated materials. These results encourage to pursue the study to other insulating crystals.

The localization tensor $\langle r_\alpha r_\beta \rangle_c$, can be computed from the periodic part of the Bloch functions $u_{nk}(\mathbf{r})$ and their first derivatives with respect to their wavevector :

$$\begin{aligned} \langle r_\alpha r_\beta \rangle_c = & \frac{V_c}{N(2\pi)^3} \int_{BZ} d\mathbf{k} \sum_{n=1}^N \left\{ \left\langle \frac{\partial u_{n\mathbf{k}}}{\partial k_\alpha} \right| \frac{\partial u_{n\mathbf{k}}}{\partial k_\beta} \right\rangle \right. \\ & \left. - \sum_{n'=1}^N \left\langle \frac{\partial u_{n\mathbf{k}}}{\partial k_\alpha} \right| u_{n'\mathbf{k}} \right\rangle \left\langle u_{n'\mathbf{k}} \left| \frac{\partial u_{n\mathbf{k}}}{\partial k_\beta} \right. \right\rangle \right\} \end{aligned} \quad (1)$$

where V_c is the volume of the primitive unit cell, N the number of doubly occupied bands and α, β are two cartesian directions. The localization tensor is a *global* quantity that characterizes the occupied Kohn-Sham manifold as a *whole* (all k-points and all bands). This statement calls for two comments. First, applications of DFT to solids often make use of the frozen-core and pseudopotential approximations, while Eq.(1) requires an all-electron calculation. Second, the behavior of core and valence electrons is treated globally while both kinds of electrons are expected to exhibit strongly different localization properties interesting to identify independently.

The localization tensor has been shown¹¹ to give a lower bound for the spread of maximally localized Wannier functions (WF) as defined by Marzari and Vanderbilt^{14,15} (hereafter

cited as MV). In order to get some insight into the physics of the chemical bonds in molecules and solids, such WF are usually constructed considering only a restricted number of electronic bands close to the Fermi level. The spread of the resulting WF is strongly dependent of the electronic states included in the minimization process. In this context, it seems interesting to try to identify the intrinsic localization of the electrons in a specific set of bands and to understand how this quantity is affected when including other bands. This would allow to solve the problem associated to the use of pseudopotentials and to characterize separately the behavior of core and valence electrons.

This paper is organized as follows. In Sec. II, we propose a decomposition of the localization tensor into contributions originating from isolated sets of bands composing the energy spectrum of a solid. Using a simple model, we then illustrate the role of the covalent interactions on the different terms of the decomposition. We also make a connection between the localization tensor and the Born effective charges and we discuss the relation between pseudopotential and all-electron calculations. In Sec. III, we give the technical details underlying our first-principles calculations and we point out the differences between our method and that applied in Ref. 11. In Sec. IV and V, we present the results obtained on two ferroelectric perovskites (BaTiO_3 and PbTiO_3) as well as on two binary oxides (BaO and $\alpha\text{-PbO}$). We investigate the variation of electron localization during the phase transitions of BaTiO_3 and show that the evolution is compatible with the electronic structure of this compound.

II. BAND BY BAND DECOMPOSITION OF THE LOCALIZATION TENSOR

A. Formalism

Contrary to the polarization and the Born effective charges, for which band-by-band decompositions have been previously reported^{16,17,18,19}, the localization tensor (Eq. (1)) involves scalar products between Bloch functions of different bands, making the identification of the contribution of isolated sets of bands less straightforward. In order to explain this fact, we have to remember that the localization tensor is related to the second moment of WF while the Born effective charges and the spontaneous polarization are linked to their first moment. From standard statistics, it is well known that these two quantities do not

add the same way : when considering two random variables x_1 and x_2 , the mean value of the sum $x_1 + x_2$ is simply the sum of the mean values while the variance of the sum is the sum of the variances *plus* an additional term, the covariance.

These considerations can be transposed in the simple context of a confined model system made of two orthonormalized states $\psi_1(x)$ and $\psi_2(x)$. The total many-body wavefunction $\Psi(x_1, x_2)$ is a Slater determinant constructed on the one-particle orbitals. The center of mass is given by the expectation value of the position operator $\hat{X} = \sum_{i=1,2} \hat{x}_i$

$$\overline{X} = \langle \Psi | \hat{X} | \Psi \rangle = \sum_{i=1,2} \langle \psi_i | \hat{x} | \psi_i \rangle \quad (2)$$

while the total spread (two times the localization tensor) is related to \hat{X}^2 ,

$$\begin{aligned} \sigma^2 &= \langle \Psi | \hat{X}^2 | \Psi \rangle - \langle \Psi | \hat{X} | \Psi \rangle^2 \\ &= \sum_{i=1,2} [\langle \psi_i | \hat{x}^2 | \psi_i \rangle - \langle \psi_i | \hat{x} | \psi_i \rangle^2] - 2 \langle \psi_1 | \hat{x} | \psi_2 \rangle \langle \psi_2 | \hat{x} | \psi_1 \rangle. \end{aligned} \quad (3)$$

We see that the first moments of the one-particle orbitals add to form the total dipole of the many-body wavefunction. On the contrary, the total spread is not equal to the sum of the individual spreads of ψ_1 and ψ_2 but involves also matrix elements of the one-particle position operator \hat{x} between ψ_1 and ψ_2 . The additional term would be absent if the many-body wavefunction was a simple product of the one-particle orbitals. It arises from the anti-symmetry requirement. In analogy with the language of statistics, we will name it the *covariance*.

Based on these arguments, we can now define a band-by-band decomposition of Eq. (1). Suppose that the band structure is formed of N_g groups labelled G_i , each of them composed of n_i bands ($i = 1, \dots, N_g$). The variance of a particular group G_i is defined as

$$\begin{aligned} \langle r_\alpha r_\beta \rangle_c(G_i) &= \frac{V_c}{n_i(2\pi)^3} \int_{BZ} d\mathbf{k} \left\{ \sum_{n \in G_i} \left\langle \frac{\partial u_{n\mathbf{k}}}{\partial k_\alpha} \right| \frac{\partial u_{n\mathbf{k}}}{\partial k_\beta} \right\rangle \right. \\ &\quad \left. - \sum_{n, n' \in G_i} \left\langle \frac{\partial u_{n\mathbf{k}}}{\partial k_\alpha} \right| u_{n'\mathbf{k}} \right\rangle \left\langle u_{n'\mathbf{k}} \left| \frac{\partial u_{n\mathbf{k}}}{\partial k_\beta} \right. \right\rangle \right\} \end{aligned} \quad (4)$$

where the sums have to be taken over the bands of group G_i . The covariance of two groups G_i and G_j ($i \neq j$) is given by the following relationship:

$$\langle r_\alpha r_\beta \rangle_c(G_i, G_j) = \frac{-V_c}{n_i n_j (2\pi)^3} \int_{BZ} d\mathbf{k} \sum_{n \in G_i} \sum_{n' \in G_j} \left\langle \frac{\partial u_{n\mathbf{k}}}{\partial k_\alpha} \right| u_{n'\mathbf{k}} \left\langle u_{n'\mathbf{k}} \left| \frac{\partial u_{n\mathbf{k}}}{\partial k_\beta} \right. \right\rangle. \quad (5)$$

Using these definitions, the total tensor, associated to the whole set of occupied bands, can be written as

$$\langle r_\alpha r_\beta \rangle_c = \frac{1}{N} \sum_{i=1}^{N_g} n_i \left\{ \langle r_\alpha r_\beta \rangle_c(G_i) + \sum_{j \neq i}^{N_g} n_j \langle r_\alpha r_\beta \rangle_c(G_i, G_j) \right\}. \quad (6)$$

The variance $\langle r_\alpha r_\beta \rangle_c(G_i)$ is intrinsic to an isolated set of bands. It is related^{10,11} to the quantity Ω_I introduced by MV through the relation

$$\Omega_I = n_i \sum_{\alpha=1}^3 \langle r_\alpha r_\alpha \rangle_c(G_i). \quad (7)$$

In a one-dimensional crystal, Ω_I is simply the lower bound of the total spread Ω of the WF³⁷,

$$\Omega = \sum_{n \in G_i} [\langle r^2 \rangle_n - \langle r \rangle_n^2], \quad (8)$$

that can be realized by choosing an adequate phase factor for the Bloch functions. In a three-dimensional crystal, it is no more possible to construct WF that are simultaneously maximally localized in all cartesian directions. It is only possible to minimize their spread in one given direction as realized for the so-called hermaphrodite orbitals introduced in Ref. 11 : these particular functions are localized (Wannier-like) in a given direction α and delocalized (Bloch-like) in the two others. The variance of a particular group of bands $\langle r_\alpha r_\alpha \rangle_c(G_i)$ is the lower bound of the *average* spread $\frac{1}{n_i} \sum_{n \in G_i} [\langle r_\alpha^2 \rangle_n - \langle r_\alpha \rangle_n^2]$ where the sum is taken over all Wannier-like functions in the unit cell belonging to group G_i . This lower bound is reached for WF that are maximally localized in direction α . The variance therefore gives some insight on the localization of the electrons within a specific set of bands taken independently. This localization is affected by the hybridizations between atomic orbitals giving rise to the formation of the considered electronic bands within the solid so that the variance can act as a probe to characterize these hybridizations.

The covariance is no more related to an isolated set of bands. It teaches us how the construction of WF including other bands can improve the localization. As discussed by MV, the definition of groups of bands in a solid is not unique and sometimes there is a doubt about which bands have to be considered together. If we consider two sets of bands G_i and G_j as one single group, its total variance is the sum of the individual variances *and*

covariances, that have to be rescaled by the number of bands in each group

$$\langle r_\alpha r_\beta \rangle_c = \frac{1}{n_i + n_j} \{ n_i [\langle r_\alpha r_\beta \rangle_c(G_i) + n_j \langle r_\alpha r_\beta \rangle_c(G_i, G_j)] + n_j [\langle r_\alpha r_\beta \rangle_c(G_j) + n_i \langle r_\alpha r_\beta \rangle_c(G_j, G_i)] \}. \quad (9)$$

Until now, we considered separately the two cartesian directions α and β . Stronger results can be obtained when diagonal elements of the localisation tensor are considered, or when this localisation tensor is diagonalized, and the eigenvalues are considered. Different inequalities can be derived. In particular, from Eq. (5), it appears that the covariances for $\alpha = \beta$ are always *negative*. This means that the diagonal elements of the full tensor are always smaller than those obtained by the sum of the diagonal variances. In other words, it is always possible to obtain more strongly localized orbitals by constructing WF considering more than one group of bands. As a consequence the covariance appears as a tool to identify which bands have to be considered together in the construction of WF in order to improve their localization.

In appendix A we give an interpretation of the variance and covariance in terms of the optical conductivity. It illustrates from a different viewpoint the influence of the fermionic nature of the electrons on the localization tensor : the appearance of the covariance in Eq. (6) is a direct consequence of the Pauli principle.

B. Simple model

In this section we will investigate a one-dimensional model system. This will help us to understand the role of the covalent interactions on the electron localization length and related quantities like the Born effective charges. We will deal with a confined system for which the localization tensor can be computed from matrix elements of the position operator and its square as described in Ref. 11.

Let us consider a diatomic molecule XY. In order to describe the chemical bonds of this model system we adopt a tight-binding scheme³³ defined by the hopping integral t and the on-site terms Δ and $-\Delta$. We will call a the interatomic distance and ψ_X, ψ_Y the s-like atomic orbitals that are used as basis functions. The hamiltonian can be rescaled by Δ

$(A=t/\Delta)$ in order to become a one parameter hamiltonian defined by

$$H = \begin{pmatrix} -1 & A \\ A & 1 \end{pmatrix}. \quad (10)$$

We further assume that ψ_X is centered at the origin, ψ_Y in a and that these two functions do not overlap at any x

$$\psi_X(x)\psi_Y(x-a) = 0. \quad (11)$$

The eigenfunctions of the hamiltonian correspond to

$$\phi_{1,2}(x) = u_{1,2}\psi_X(x) + v_{1,2}\psi_Y(x-a) \quad (12)$$

where the coefficients $u_{1,2}$ and $v_{1,2}$ can be expressed in terms of the bond polarity³³ α_p ($\alpha_p = \frac{1}{\sqrt{1+A^2}}$):

$$\begin{aligned} u_1 &= \sqrt{\frac{1+\alpha_p}{2}}, & v_1 &= \sqrt{\frac{1-\alpha_p}{2}} \\ u_2 &= \sqrt{\frac{1-\alpha_p}{2}}, & v_2 &= -\sqrt{\frac{1+\alpha_p}{2}}. \end{aligned} \quad (13)$$

In order to see the meaning of the different terms appearing in the band by band decomposition of the localization tensor and the Born effective charges let us first consider the molecular orbitals independently.

The variance of state ϕ_1 can be computed from the coefficients u_1 and v_1 . It writes

$$\langle x^2 \rangle_c(1) = \sigma_X^2 \frac{1 + \alpha_p}{2} + \sigma_Y^2 \frac{1 - \alpha_p}{2} + \frac{a^2 A^2}{4(1 + A^2)} \quad (14)$$

where σ_X^2 and σ_Y^2 are the second central moments of ψ_X and ψ_Y . The variance of ϕ_2 is given by a similar expression. This quantity is composed of three positive terms that summarize the mechanisms that are able to delocalize the electrons with respect to the atomic orbitals. On one hand, the electronic cloud on a particular atom is not a delta-Dirac function but presents a degree of delocalization related to σ_X^2 and σ_Y^2 (first and second term). When the state ϕ_1 is made entirely of ψ_X , that is, when α_p equals one, the localization length is correctly equal to σ_X^2 (first term). Incorporating more ψ_Y changes the localization length in proportion of α_p (the balance between first and second terms). On the other hand, the electrons can occupy two sites X and Y that are separated by a distance a (third term). This term scales as a^2 . Even a small covalent interaction is thus able to induce an important delocalization if it acts on a sufficiently large distance.

The Born effective charge of atom X is defined as the derivative of the dipole moment p with respect to a . This dipole moment is the sum of the nuclear and static electronic charges multiplied by the interatomic distance. The contribution coming from the electrons occupying state ϕ_1 is equal to

$$p_1 = -2eu_1^2a = -e(1 + \alpha_p)a \quad (15)$$

where e is the module of the electronic charge. The derivative of Eq. (15) with respect to a gives the contribution of these electrons to the total effective charge

$$Z_{X,1}^* = \frac{\partial p_1}{\partial a} = -e(1 + \alpha_p) + ea \frac{A}{(1 + A^2)^{3/2}} \frac{\partial A}{\partial a}. \quad (16)$$

The first term is the (static) effective atomic charge³³ of atom X while the second term represents an additional dynamical contribution due to a transfer on electrons between X and Y during a relative atomic displacement. The contribution of the electrons occupying state ϕ_2 is given by a similar expression

$$Z_{X,2}^* = \frac{\partial p_2}{\partial a} = -e(1 - \alpha_p) - ea \frac{A}{(1 + A^2)^{3/2}} \frac{\partial A}{\partial a}. \quad (17)$$

This simple model illustrates how both the variance of the localization tensor and the Born effective charges depend on the covalent interactions defined by the parameter A . The variance is a *static* quantity depending on the amplitude of the covalent interactions only while the the Born effective charges are *dynamical* quantities that also depend on the variations of these interactions during a relative atomic displacement.

If we now consider the states ϕ_1 and ϕ_2 as a single group we have to add their variances and covariances to get the whole localization tensor. The covariance reduces to

$$\langle x^2 \rangle_c(1, 2) = \frac{-a^2 A^2}{4(1 + A^2)}. \quad (18)$$

By adding this covariance to the variance in Eq. (14), we remove in some sense the delocalization induced by the covalent interactions. The total localization tensor becomes independent of the hopping A and the interatomic distance a . It reduces to the mean spread of the atomic orbitals ψ_X and ψ_Y :

$$\langle x^2 \rangle_c = \frac{\sigma_X^2 + \sigma_Y^2}{2}. \quad (19)$$

Eq. (19) defines the mean spread of the WF constructed as linear combinations of ϕ_1 and ϕ_2 that minimize the spread functional Ω (see Eq. (8)). As shown by MV, these WF diagonalize

the position operator \hat{x} projected on the subspace of occupied states. They are thus equal to the atomic orbitals since the hypothesis of zero overlap (Eq. (11)) implies $\langle \psi_X | \hat{x} | \psi_Y \rangle = 0$.

The total Born effective charge of atom X can be obtained by adding the nuclear charge $Z_{core}^* = 2e$ to the terms (16) and (17). It is easy to check that for this model Z_X^* is equal to zero. This result can be interpreted in two ways. The point of view usually adopted is to say that the two molecular orbitals are of the opposite polarity so that the total dipole of the molecule vanishes. Based on the results of the preceding paragraph, we can also affirm that each maximally localized WF is confined on a single atom so that no interatomic charge transfer can take place.

This result suggests that the variance gives more informations about the localization of electrons of particular chemical bonds than the total localization tensor. It also illustrates the observation of Ghosez *et al.*^{17,18} that anomalous effective charges mainly come from hybridizations between occupied and unoccupied states. In fact, the different chemical bonds generate opposite effects so that a net charge transfer is possible only if some of them are unoccupied.

In summary, we have illustrated the mechanisms that govern the variance of the localization tensor and the Born effective charges in the particular case of a one dimensional model system. The observations made in this section give us an intuitive understanding of how delocalized electrons can generate *anomalous* effective charges. Hybridizations between occupied states generate opposite effects that tend to cancel out when they are summed. Because of the simplicity of the above adopted picture, we have however to be careful when we apply this model to real materials. First, we considered only hybridizations between two types of atomic orbitals, while the chemical bonds in real systems generally result from more complicated interactions. In particular, we neglected on-site hybridizations that are also able to generate *anomalous* effective charges but that induce a stronger localization on the electronic cloud. Second, the hypothesis of zero overlap (11) is not always fulfilled so that maximally localized WF constructed on the whole set of occupied states generally not reduce to the atomic orbitals. Nevertheless, this simple model will allow us to interpret some results in Sections IV and V.

C. Pseudopotentials

As mentioned in the introduction, there is a fundamental problem in the computation of the total localization tensor when pseudopotentials are used. This is due to the fact that the localization tensor is related to the bands of the system as a whole : first, there is no cancellation between the core electrons and the nuclear charge, as it is the case in the computation of the total polarization; second, the localization tensor is a kind of mean over all bands, that combines strongly localized (core) states, and weakly localized (valence) states. This is clearly seen in Eq.(1), where the number of bands explicitly appears both as the denominator of the prefactor and in the two summations. The band-by-band decomposition allows us to overcome this problem partly, by focusing only on the variances of isolated groups of bands. Thanks to Eq. (9) it is also possible to get some insight into the physics of the all-electron localization tensor when pseudopotentials are used. In this section, we focus on the diagonal elements of the electron localization tensor $\alpha = \beta$ (of course, any direction can be chosen as α).

In an all-electron calculation, let us consider separately two sets of bands: core bands (labelled as 'co'), and valence bands (labelled as 'va'). The total localization tensor can be obtained from the localization tensors of each group of bands, combined with the covariance between the two groups of bands:

$$\langle r_\alpha r_\alpha \rangle_c = \frac{1}{n_{co} + n_{va}} \{ n_{co} \langle r_\alpha r_\alpha \rangle_c (co) + n_{va} \langle r_\alpha r_\alpha \rangle_c (va) + 2n_{co}n_{va} \langle r_\alpha r_\alpha \rangle_c (co, va) \}. \quad (20)$$

Both variances $\langle r_\alpha r_\alpha \rangle_c (co)$ and $\langle r_\alpha r_\alpha \rangle_c (va)$ are positive quantities. The covariance times the product of the number of bands $n_{co}n_{va} \langle r_\alpha r_\alpha \rangle_c (co, va)$, a negative quantity, must always be smaller in magnitude than each of the related variances multiplied by the corresponding number of bands. This translates to bounds on the diagonal elements of the total localization tensor :

$$\frac{|n_{va} \langle r_\alpha r_\alpha \rangle_c (va) - n_{co} \langle r_\alpha r_\alpha \rangle_c (co)|}{n_{co} + n_{va}} \leq \langle r_\alpha r_\alpha \rangle_c \leq \frac{n_{va} \langle r_\alpha r_\alpha \rangle_c (va) + n_{co} \langle r_\alpha r_\alpha \rangle_c (co)}{n_{co} + n_{va}}. \quad (21)$$

In the frozen-core approximation, $\langle r_\alpha r_\alpha \rangle_c (co)$ can be obtained from separate all-electron calculations for each atom of the system. The localization tensor of the valence bands is (likely) computed accurately in the pseudopotential approximation : the spread of the Wannier functions should be quite similar if estimated from all-electron valence wavefunctions or from pseudo-wavefunctions.

Thus, a *bound* on the diagonal elements of the localization tensor *can be computed* from the atomic wavefunctions of the core electrons and the pseudo-valence wavefunctions. In order to compute the covariance more accurately it is necessary to reconstruct the all-electron wavefunctions. This could be done following the ideas exposed in Ref. 34.

III. METHOD AND IMPLEMENTATION

In the remaining part of this paper, we apply the previous formalism to various oxides. The electronic wavefunctions are obtained within DFT^{12,13} and the local density approximation (LDA) thanks to the ABINIT²¹ package. At variance with a previous work on semiconductors¹¹, the first derivatives of the wave functions with respect to their wavevector are not computed from finite differences but from a linear-response approach²⁶ within the parallel-transport gauge. The wave functions are further transformed to the diagonal gauge¹⁹. Both ground-state and first-order wavefunctions are expanded in plane waves up to a kinetic-energy cutoff of 45 Hartree. Integrations over the BZ are replaced by sums over a $8 \times 8 \times 8$ mesh of special k-points²⁷. With these parameters, the convergence of the localization tensor for the investigated compounds is better than 10^{-3} Bohr². The ionic-core electron potentials of the Ba, Pb, Ti and O atoms are replaced by ab initio, separable, extended norm-conserving pseudopotentials, as proposed by M. Teter²⁸. Ba 5s, 5p and 6s electrons, Pb 6s, 5d and 6p electrons, Ti 3s, 3p and 3d electrons, O 2s and 2p electrons are considered as valence states. Beside calculating the localization tensor on bulk-materials, we also computed it on the isolated atomic systems Ba²⁺, Pb²⁺ and O by placing each atom at the origin of a periodic supercell of 20 Bohrs.

As shown by Sgariollo *et al.*¹¹, the localization tensor and thus the variances and covariances, are real. Moreover, they are obviously symmetric in α and β . Consequently there exists a set of cartesian axes where they are diagonal and their eigenvalues are also real numbers. In the discussion of our results we will always work in this particular frame so that we do not need to consider the off-diagonal elements of the localization tensor.

IV. RESULTS

A. Structural and electronic properties

We will consider the two binary oxides BaO and α -PbO as well as the ferroelectric perovskites BaTiO₃ and PbTiO₃. BaO has a rocksalt structure while the tetragonal α phase of lead oxide is formed of parallel layers of Pb and O atoms. BaTiO₃ and PbTiO₃ have a high-temperature cubic perovskite structure with five atoms per unit cell. As the temperature is lowered, the former compound undergoes a sequence of three ferroelectric phase transitions transforming to tetragonal, orthorhombic and rhombohedral structures while the latter compound only undergoes one single transition from the cubic to the tetragonal phase. We will consider explicitly the cubic, tetragonal and rhombohedral phases of BaTiO₃ as well as the cubic phase of PbTiO₃.

The electronic structures of these compounds have been previously studied^{16,29,31,32} and are illustrated in Fig. 1. They are formed of well separated groups of bands. Each of them has a marked dominant orbital character and can be labeled by the name of the atomic orbital that mainly composes the energy state in the solid. The bands at the Fermi level are mainly composed of O 2p states that show significant interactions with other atomic orbitals like the well known O 2p-Ti 3d hybridization in BaTiO₃ and PbTiO₃. The bandstructures in the ferroelectric phases of BaTiO₃ are similar to that of the cubic phase. The phase transitions principally affect the bandgap and the spread of the O 2p bands while the positions of the deeper lying bands remain quite constant. The main difference in the electronic structures of BaO and BaTiO₃ on one hand and PbO and PbTiO₃ on the other hand comes from the presence or absence of Pb 6s electrons (that form the so called lone-pair in PbO). These electrons show a strong hybridization with the O 2p states. As a consequence the O 2p and Pb 6s bands are degenerate at the *R* point in PbTiO₃ and around the *Z* point in PbO. Consequently, we have to consider them as one single group of bands in the decomposition of the localization tensor.

B. Localization tensor and Born effective charges

As the total localization tensor is meaningless in pseudopotential calculations that do not include covariances with the core states, we focus on the variances of the different groups

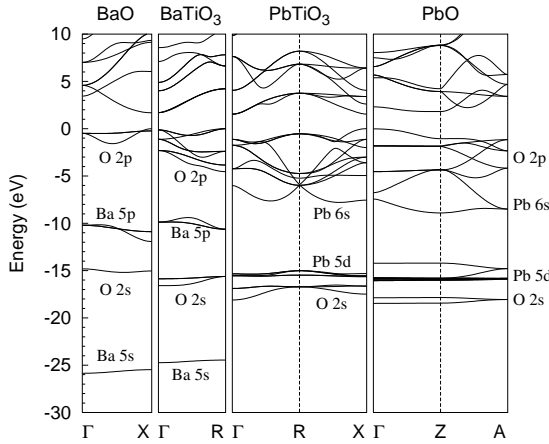


FIG. 1: Band structures of BaO, cubic BaTiO₃, cubic PbTiO₃ and α -PbO.

of bands. The values can be found in the Tables I and II where they are compared to the variances of the dominant atomic orbitals. We do not report any values associated to the deepest lying Ti 3s and Ti 3p bands although they have been included in our pseudopotential calculation. Their variances are in fact close to the atomic ones and they do not show any sizeable covariance with other bands in both BaTiO₃ and PbTiO₃.

TABLE I: Variances (Bohr²) of the Ba 5s, O 2s, Ba 5p and O 2p bands for the isolated atomic systems Ba²⁺ and O, BaO and the cubic (C), tetragonal (T) and rhombohedral (R) phases of BaTiO₃.

System	Str.	Element	Band			
			Ba 5s	O 2s	Ba 5p	O 2p
Atom	—	$\langle r^2 \rangle_c$	1.011	0.929	1.370	—
BaO	—	$\langle r^2 \rangle_c$	1.065	1.552	2.023	2.199
BaTiO ₃	C	$\langle r^2 \rangle_c$	1.091	0.950	2.189	1.875
	T	$\langle r_{\perp}^2 \rangle_c$	1.091	0.945	2.180	1.852
		$\langle r_{\parallel}^2 \rangle_c$	1.088	0.965	2.175	1.842
	R	$\langle r_{\perp}^2 \rangle_c$	1.092	0.963	2.196	1.862
		$\langle r_{\parallel}^2 \rangle_c$	1.092	0.949	2.189	1.804

In the cubic crystals BaO, BaTiO₃ and PbTiO₃ as well as in the atomic systems, the

TABLE II: Variances (Bohr²) of the O 2s, Pb 5d and Pb 6s + O 2p bands in PbTiO₃, α -PbO and for the isolated atomic systems Pb²⁺ and O.

System	Element	Band		
		O 2s	Pb 5d	Pb 6s + O 2p
Atom	$\langle r^2 \rangle_c$	0.929	0.657	—
PbTiO ₃	$\langle r^2 \rangle_c$	1.874	1.490	1.749
PbO	$\langle r_{\perp}^2 \rangle_c$	2.234	1.142	2.178
	$\langle r_{\parallel}^2 \rangle_c$	1.724	0.990	1.968

reported tensors are isotropic so that we only mention their principal values $\langle r^2 \rangle_c$. This is no more true in the ferroelectric phases of BaTiO₃ where a weak anisotropy can be observed. The tensors have an uniaxial character as the corresponding dielectric ones: they are diagonal when expressed in the principal axes and the elements $\langle r_{\perp}^2 \rangle_c$ and $\langle r_{\parallel}^2 \rangle_c$ refer to cartesian directions perpendicular and parallel to the optical axis (that has the direction of the spontaneous polarization). A much stronger anisotropy is observed in α -PbO where the localization tensor has the same symmetry as in the ferroelectric phases of BaTiO₃. Due to its particular structure formed of atomic Pb-O planes the electrons of each group of bands are more delocalized in a direction parallel ($\langle r_{\parallel}^2 \rangle_c$) to the atomic planes³⁸ than perpendicular ($\langle r_{\perp}^2 \rangle_c$) to them. This observation agrees with our intuitive picture that the covalent interactions between atoms inside a layer are stronger than between atoms of different layers.

Examining the variances of the different groups of bands we see that the Ba 5s electrons show a similar degree of localization both in BaO and BaTiO₃ also equivalent to that of the corresponding atomic orbital. On the contrary, the O 2s electrons behave differently in the materials under investigation: in BaTiO₃, their variance is close to the atomic one while they show a significant larger delocalization in the three other compounds. It is in fact surprising to see the degree of delocalization of the inner bands like the O 2s, Ba 5p or Pb 5d bands. In some cases like BaTiO₃, the electrons of these bands are even more strongly delocalized than those of the bands at the Fermi level. These results suggest that the corresponding atomic orbitals are chemically not inert but present non negligible covalent interactions. An interesting observation can be made for the O 2s and Pb 5d bands in PbTiO₃ and α -PbO. The delocalization induced by the covalent interactions that generate these bands

tends to disappear when we consider them as one single group. In order to compute the variance of the whole O 2s and Pb 5d bands, we have to use Eq. (9). As an example let us consider PbTiO_3 . The different elements can be summarized in a matrix where the diagonal elements are the variances (Bohr^2) and the off-diagonal elements the covariances (Bohr^2) of the individual groups

$$\begin{pmatrix} 1.874 & -0.240 \\ -0.240 & 1.490 \end{pmatrix}.$$

The total variance of the (O 2s + Pb 5d) group considered as a whole reduces to 0.734 Bohr^2 . For $\alpha\text{-PbO}$, we obtain similar values of 0.732 Bohr^2 for $\langle r_{\perp}^2 \rangle_c$ and 0.701 Bohr^2 for $\langle r_{\parallel}^2 \rangle_c$. These values can be compared to the mean spread of the atomic orbitals $\frac{1}{6}(0.929 + 5 \times 0.657) = 0.702 \text{ Bohr}^2$.

The results presented above suggest that inner orbitals like O 2s, Ba 5p or Pb 5d are chemically not inert in the materials under investigation. This observation seems in contradiction with the conclusions drawn from partial density of states analysis³¹ that these states are rather inert. Nevertheless the inspection of the Born effective charges in BaO or BaTiO_3 ^{16,18} confirms our observations that will now be illustrated for $\alpha\text{-PbO}$ and PbTiO_3 . This points out that the global shape of the bandstructure is less sensitive to the underlying covalent interactions than the variance of the localization tensor or the Born effective charges.

In order to investigate the connection between the localization tensor and the Born effective charges we report in Table III the band by band decomposition of Z_{Pb}^* in PbTiO_3 and $\alpha\text{-PbO}$. In the perovskite, this tensor is isotropic while in $\alpha\text{-PbO}$ it has the same symmetry as the localization tensor. The contribution of each group of bands has been separated into a reference nominal value and an *anomalous* charge³⁹. For $\alpha\text{-PbO}$, we observe the same anisotropy as for the localization tensor: the covalent interactions inside an atomic layer ($Z_{Pb\perp}^*$) generate larger *anomalous* contributions than the interactions involving atoms of different layers ($Z_{Pb\parallel}^*$). By looking at the O 2s and Pb 5d bands we see that they generate important anomalous charges that confirm our observations concerning the variances of these bands. Interestingly, in both materials these contributions cancel out when they are summed. We observe thus the same tendencies for the Born effective charges and the localization tensor: the effects induced by the covalent interactions between inner orbitals tend to disappear when the resulting bands are considered together.

TABLE III: Band by band decomposition of the Born effective charges (a. u. of charge) in PbTiO_3 and $\alpha\text{-PbO}$. The contributions have been separated into a reference nominal value and an *anomalous* charge.

Band	Z_{Pb}^*	$Z_{Pb\perp}^*$	$Z_{Pb\parallel}^*$
Core	14.00	14.00	14.00
O 2s	$0 + 3.47$	$0 + 1.89$	$0 + 0.26$
Pb 5d	$-10 - 3.36$	$-10 - 1.80$	$-10 - 0.40$
Pb 6s + O 2p	$-2 + 1.78$	$-2 + 1.06$	$-2 + 0.48$
Tot.	$2 + 1.89$	$2 + 1.15$	$2 + 0.34$

V. DISCUSSIONS

Based on the simple model exposed in Sec. II B we can suggest the following mechanism to explain the results presented in the preceeding section. The atomic orbitals O 2s and Pb 5d (for which the hypothesis of zero overlap (11) is reasonable) present weak covalent interactions that generate the corresponding energy bands in PbTiO_3 and $\alpha\text{-PbO}$. When we construct maximally localized WF for each individual group, the resulting orbitals are delocalized on Pb and O atoms so that during an atomic displacement an interatomic transfer of charges – generating *anomalous* Born effective charges – is possible. The fact that the variance of the global (O 2s + Pb 5d) group of bands is close to the mean spread of the atomic orbitals suggests that the maximally localized WF constructed on these bands are similar to the original atomic orbitals. In other words, they are confined on a single atom. This confinement also suppresses the interatomic charge transfer so that the anomalous charges disappear. We can make similar observations for the Ba 5p and O 2s bands in BaO and BaTiO_3 , although, in the latter compound, the cancellation in the Born effective charges and the variance is not as complete as in the three remaining ones. This suggests that in the lead oxides as well as in BaO, the inner bands Pb 5d and O 2s (resp. Ba 5p and O 2s) mainly result from hybridizations between two types of atomic orbitals. At the opposite, in BaTiO_3 the Ba 5p and O 2s bands are formed of more than two types of atomic orbitals.

Looking now at the bands at the Fermi level, we see that their variance is significantly

larger in BaO and α -PbO than in the corresponding perovskites and that it remains nearly constant in the different phases of BaTiO₃. This latter observation seems surprising for two reasons. (i) The LDA bandgap presents drastic changes when passing from the cubic (1.72 eV) to the rhombohedral (2.29 eV) phase. This increase suggests a much stronger localization of the O 2p electrons in the ferroelectric phases. (ii) The giant Born effective charges observed in the paraelectric phase^{17,18} imply an important reorganization of the electronic cloud during an atomic displacement. It appears surprising that this reorganization has such small effects on the localization tensor. These small variations are not restricted to BaTiO₃ but similar observations have been made in other ferroelectric compounds like LiNbO₃³⁵.

Considering point (i), we note that the correlation between the bandgap and the localization tensor is not as tight as one might think. The variance of the O 2p bands for instance is significantly larger in BaO than in BaTiO₃ in spite of the fact that its LDA bandgap (1.69 eV) is close to the gap in the cubic phase of BaTiO₃.

Considering point (ii), we note that it is possible to have an important reorganization of the electronic charge *without* affecting the localization tensor a lot. Following the ideas of the Harrison model³³, the giant effective charges in perovskite ferroelectrics result from dynamical orbital hybridizations changes generating interatomic transfers of charges. In Fig. 2 (a) we have drawn schematically an O centered WF in the cubic phase of BaTiO₃ along a Ti - O chain. Due to the O 2p - Ti 3d hybridization, this WF has a finite probability on the neighbouring Ti₁ and Ti₂ atoms. According to the Harrison model, a fraction of

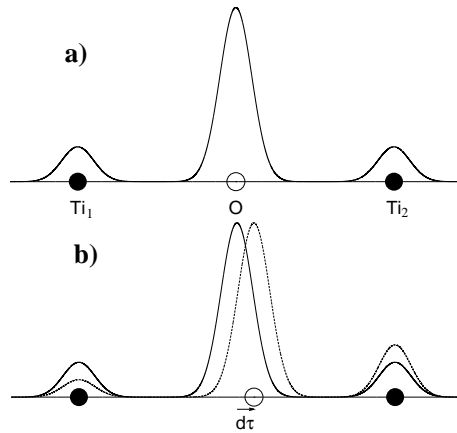


FIG. 2: Oxygen centered WF in the cubic phase (solid line) of BaTiO₃ (a) and its variation during the transition to the tetragonal phase (dashed line) (b).

electrons is transferred from Ti_1 to Ti_2 during a displacement $d\tau$ of the O atom (Fig. 2 (b)). Even if the quantity of charges involved in this process is small, the large scale on which this transfer takes place (of the order of the lattice parameter) implies a shift of the WF center larger than the underlying atomic displacement and explains the *anomalous effective charges*. During the transition from the cubic to the tetragonal phase, the central O atom is displaced by few percents of the lattice constant a ($\frac{d\tau}{a} = 0.045$) with respect to Ti_1 and Ti_2 . The resulting shift of the WF center generates the spontaneous polarization in the ferroelectric phase.

Based on this simple picture the origin of the small variations of the O 2p variance during the phase transitions becomes more obvious: When the electrons are transferred from Ti_1 to Ti_2 their distance to the initial WF center remains unaffected and their distance to the displaced WF center slightly decreases due to its shift towards Ti_2 . Mathematically speaking, due to the fact that the variations do not depend on the direction of the atomic displacement, they are of the second order in $\frac{d\tau}{a}$.

In order to get a numerical estimate of the charges transferred during this process and its impact on the localization tensor we can consider a one dimensional model WF whose square is the sum of three delta-Dirac functions

$$|W_n(x)|^2 = \frac{1}{2} \left\{ \frac{2 - Z'_O}{2} [\delta(x - a) + \delta(x + a)] + Z'_O \delta(x) \right\}. \quad (22)$$

This model only takes into account the delocalization of the electrons on different atoms (third term of Eq. (14)) while it completely neglects the delocalization of the electronic cloud on the individual atoms (first and second term of Eq. (14)). In this particular case we can identify the localization tensor to the second moment of the WF. This is no more true in a real, three dimensional crystal. In BaTiO_3 for instance, the O 2p group contains 9 different WF per unit cell located on three different O atoms. These WF extend in different spatial directions so that their *average* spread in the x -direction is lower than the spread of one single WF as the one shown in Fig. 2.

In Eq. (22), Z'_O represents the probability of the electrons to be found on the O atom. It can be computed from the value of the O 2p variance in the paraelectric phase of BaTiO_3 and the lattice constant a using the relation $\int x^2 |W_n(x)|^2 dx = \langle r^2 \rangle_{c,O2p}$. This yields $Z'_O = 1.73$. This quantity allows an estimate of the static charge of the O atom in BaTiO_3 by subtracting three times Z'_O from the charge due to the nucleus and the core electrons O 1s and O 2s.

This yields $Z_{O,st} = 4 - 3 \cdot 1.73 = -1.19$ e.

When the O atom is displaced, the shift of the WF center is directly related to the quantity of charges ε transferred from Ti_1 to Ti_2 . The value of ε can be computed from the value of the effective charge generated by the O 2p electrons ($Z_{O2p}^* = -9.31$) in the cubic phase¹⁷ by taking into account that the *anomalous* charges are generated by three WF located on the same O atom¹⁵. To get the polarization due to one single WF, we have to divide this quantity by 3 since each of them brings a similar contribution to Z_{O2p}^* . In the tetragonal phase, the model WF writes

$$|W_n(x)|^2 = \frac{1}{2} \left\{ \frac{2 - Z'_O - \varepsilon}{2} \delta(x + a) + Z'_O \delta(x - d\tau) + \frac{2 - Z'_O + \varepsilon}{2} \delta(x - a) \right\}. \quad (23)$$

By identifying twice its first moment to $Z_{O2p}^* d\tau / 3$ one gets $\varepsilon = 0.0614$ at the transition from the cubic to the tetragonal state. It implies a decrease in the spread of the model WF of 0.18 Bohr².

This variation is larger than the observed one (0.023 Bohr²). Part of the discrepancy is probably due to the fact that we considered Z_{O2p}^* to be constant along the path of atomic displacement from the paraelectric to the ferroelectric phase. Using the value of Z_{O2p}^* in the tetragonal phase we obtain a value of 0.0467 for ε while the variance decreases of 0.12 Bohr². Moreover, one has to bear in mind that the localization tensor in BaTiO_3 is an average value that has to be taken over 9 WF. Six of them are centered on O atoms that lie in a plane perpendicular to the direction of the spontaneous polarization. They are probably less affected by the phase transition. As a consequence, the variation of the WF located on the remaining O atom (the one represented on Fig. 2) is expected to be larger than the variation of the localization tensor.

In summary, even if there is no formal connection between the real WF in BaTiO_3 and Eq. (22), this simple model shows that small variations of the localization tensor are compatible with giant effective charges and their interpretation in terms of the Harrison model. As illustrated with the model WF, the transfer of charges along the Ti–O chains only implies a slight decrease in the spread of one single WF. This *decrease* is expected to be larger than the decrease in the variance because this latter quantity is an average value over 9 WF that are not modified to the same extent during the phase transition.

VI. CONCLUSIONS

Using a plane wave-pseudopotential approach to DFT we computed the electron localization tensor for various oxides. Our study was based on the work on semiconductors performed by Sgarirovello and co-workers but used linear-response techniques to compute the first-order wavefunctions.

In order to investigate the properties of electrons occupying individual groups of bands independently, we first set-up a band by band decomposition of the localization tensor. In analogy with the field of statistics we had to distinguish between variance and covariance in this decompositon. The significance of these new concepts was illustrated in terms of WF and explained on a simple model. The variance allows to get some insight into the hybridizations of atomic orbitals. The covariance can be useful to help constructing maximally localized WF: It identifies the bands that have to be considered together in order to improve their localization. We also made a connection between the localization tensor and the Born effective charges and we discussed the difference between all-electron and pseudopotential calculations.

We applied these techniques to binary oxides (BaO and α -PbO) as well as perovskite ferroelectrics (BaTiO₃ and PbTiO₃). By considering first the electrons of the inner bands we showed that some of them present a strong delocalization with respect to the situation in an isolated atom. This observation suggests that the underlying atomic orbitals are chemically not inert but present non negligible covalent interactions. This fact had been confirmed from an inspection of the Born effective charges.

Finally, the variations of the O 2p variance during the ferroelectric phase transitions of BaTiO₃ were found to be very small. This surprizing result was explained in terms of the electronic structure of this compound as it is interpreted in the Harrison model.

We think that, when combined with Born effective charges, the band-by-band decomposition of the localization tensor could provide a powerful tool for the qualitative characterization of bonds in solids. However, more studies are needed, for different classes of materials, in order to make it fully effective.

Acknowledgments

M. V. and X. G. are grateful to the National Fund for Scientific Research (FNRS-Belgium) for financial support. Ph. G. acknowledges support from FNRS-Belgium (grant 9.4539.00) and the Université de Liège (Impulsion grant). This work was supported by the Volkswagen-Stiftung (www.volkswarenstiftung.de) within the program "Complex Materials: Cooperative Projects of the Natural, Engineering, and Biosciences" with the title: "Nano-sized ferroelectric Hybrids" under project number I/77 737. It was also supported by the Communauté Française through the "Action de Recherche Concertée: Interaction Electron-Vibration dans les nanostructures", and the Belgian Federal Government, through the PAI/IUAP P5 "Quantum Phase Effects in Nanostructured Materials"

- ¹ W. Kohn, Phys. Rev. **133**, A171 (1964).
- ² R. D. King-Smith and D. Vanderbilt, Phys. Rev. B **47**, 1651 (1993).
- ³ D. Vanderbilt and R. D. King-Smith, Phys. Rev. B **48**, 4442 (1993).
- ⁴ R. Resta, Rev. Mod. Phys. **66**, 899 (1994).
- ⁵ G. Ortiz and R. M. Martin, Phys. Rev. B **49**, 14202 (1994).
- ⁶ R. Resta, Phys. Rev. Lett. **80**, 1800 (1998).
- ⁷ R. Resta and S. Sorella, Phys. Rev. Lett. **82**, 370 (1999).
- ⁸ A. A. Aligia and G. Ortiz, Phys. Rev. Lett. **82**, 2560 (1999).
- ⁹ R. Resta, J. Phys.: Condens. Matter **14**, R625 (2002).
- ¹⁰ I. Souza, T. Wilkens and R. M. Martin, Phys. Rev. B **62**, 1666 (2000).
- ¹¹ C. Sgiarollo, M. Peressi and R. Resta, Phys. Rev. B **64**, 115202 (2001).
- ¹² P. Hohenberg and W. Kohn, Phys. Rev. **136**, B864 (1964).
- ¹³ W. Kohn and L. J. Sham, Phys. Rev. **140**, A1133 (1965).
- ¹⁴ N. Marzari and D. Vanderbilt Phys. Rev. B **56**, 12847 (1997).
- ¹⁵ N. Marzari and D. Vanderbilt, in *First-Principles Calculations for Ferroelectrics*, edited by R. E. Cohen, AIP Conf. Proc. No. 436 (AIP, Woodbury, 1998), p. 146.
- ¹⁶ M. Posternack, A. Baldereschi, H. Krakauer and R. Resta, Phys. Rev. B **55**, 15983 (1997).
- ¹⁷ Ph. Ghosez, J.-P. Michenaud and X. Gonze, Phys. Rev. B **58**, 6224 (1998).

¹⁸ Ph. Ghosez, X. Gonze, Ph. Lambin and J.-P. Michenaud, Phys. Rev. B **51**, 6765 (1995).

¹⁹ Ph. Ghosez and X. Gonze, J. Phys.: Condens. Matter **12**, 9179 (2000).

²⁰ X. Gonze, Phys. Rev. A **52**, 1096 (1995).

²¹ ABINIT is a common project of the Université Catholique de Louvain, Corning Incorporated, and other contributors (URL <http://www.abinit.org>). It relies on an efficient Fast Fourier Transform algorithm²² for the conversion of wavefunctions between real and reciprocal space, on the adaptation to a fixed potential of the band-by-band conjugate gradient method²³ and on a potential-based conjugated-gradient algorithm for the determination of the self-consistent potential²⁴. In addition to usual ground-state calculations it allows linear-response computations of the phonon frequencies, Born effective charges and dielectric constants^{25,26}.

²² S. Goedecker, SIAM J. on Scientific Computing **18**, 1605 (1997).

²³ M. C. Payne, M. P. Teter, D. C. Allan, T. A. Arias et J. D. Joannopoulos, Rev. Mod. Phys **64**, 1045 (1992).

²⁴ X. Gonze, Phys. Rev. B **54**, 4383 (1996).

²⁵ X. Gonze and C. Lee, Phys. Rev. B **55**, 10355 (1997).

²⁶ X. Gonze, Phys. Rev. B **55**, 10337 (1997).

²⁷ H. J. Monkhorst and J. D. Pack, Phys. Rev. B **13**, 5188 (1976).

²⁸ M. P. Teter, Phys. Rev. B **48**, 5031 (1993).

²⁹ Ph. Ghosez, X. Gonze and J.-P. Michenaud, Ferroelectrics **220**, 1 (1999).

³⁰ P. Pertosa and F. M. Michel-Calendini, Phys. Rev. B **17**, 2011 (1978).

³¹ G. W. Watson, S. C. Parker and G. Kresse, Phys. Rev. B **59**, 8484 (1999).

³² R. D. King-Smith and D. Vanderbilt, Phys. Rev. B **49**, 5828 (1994).

³³ Harrison W. A., “Electronic structure and the properties of solids”, W. H. Freeman and Co, San Francisco, 1980.

³⁴ C. B. Van de Walle and P. E. Blöchl, Phys. Rev. B **47**, 4244 (1993).

³⁵ M. Veithen, X. Gonze and Ph. Ghosez, to appear in *Fundamental Physics of Ferroelectrics*, edited by R. E. Cohen, AIP Conf. Proc. (Washington 2002).

³⁶ F. Bassani and G. Pastori Parravicini, *Electronic States and Optical Transitions in Solids* (Pergamon, Oxford, 1975).

³⁷ $\langle \dots \rangle_n$ represents the expectation value over the n^{th} occupied Wannier function in the unit cell

³⁸ In α -PbO, the optical axis is perpendicular to the atomic layers.

³⁹ The Born effective charges are in general compared to an isotropic nominal value that is the charge expected in a purely ionic compound. All deviations with respect to this reference nominal value are referred to as *anomalous*.

APPENDIX A: OPTICAL CONDUCTIVITY

The optical conductivity (imaginary part of the optical dielectric tensor) of a given material is related to its absorption coefficient, the probability of the valence electrons to perform optical transitions to the *unoccupied* conduction bands under the influence of an electromagnetic field. If we consider only "vertical" band-to-band transitions (thus neglecting elementary excitations like the electron-hole interaction or the electron-phonon coupling) this quantity writes in the dipolar approximation³⁶

$$\varepsilon''_{\alpha\beta}(\omega) = \frac{4\pi^2 e^2}{m^2 \omega^2 \hbar} \sum_{n=1}^N \sum_{m=N+1}^{\infty} \int_{BZ} \frac{2d\mathbf{k}}{(2\pi)^3} p_{nm}^{\alpha}(\mathbf{k}) p_{mn}^{\beta}(\mathbf{k}) \delta(\omega_{mn}(\mathbf{k}) - \omega) \quad (\text{A1})$$

where m is the electron mass, $\mathbf{p}_{nm}(\mathbf{k}) = -i\hbar\langle\psi_{n\mathbf{k}}|\nabla\psi_{m\mathbf{k}}\rangle$ and $\hbar\omega_{mn}(\mathbf{k}) = \varepsilon_{m\mathbf{k}} - \varepsilon_{n\mathbf{k}}$. The matrix elements of the momentum operator can equivalently be expressed as $\mathbf{p}_{nm}(\mathbf{k}) = -m\omega_{nm}(\mathbf{k})\langle u_{n\mathbf{k}}|\partial_{\mathbf{k}}u_{m\mathbf{k}}\rangle$.

It has been shown by Souza, Wilkens and Martin¹⁰ that ε'' is related to the localization tensor by the relation

$$\int_0^{\infty} \varepsilon''_{\alpha\beta}(\omega) d\omega = \frac{8\pi^2 e^2 N}{\hbar V_c} \langle r_{\alpha} r_{\beta} \rangle_c. \quad (\text{A2})$$

In order to see the effect of the band by band decomposition, we will write ε'' as

$$\varepsilon''_{\alpha\beta}(\omega) = \sum_{i=1}^{N_g} \left\{ \varepsilon''_{\alpha\beta}(\omega; G_i) + \sum_{j \neq i}^{N_g} \varepsilon''_{\alpha\beta}(\omega; G_i, G_j) \right\} \quad (\text{A3})$$

where

$$\varepsilon''_{\alpha\beta}(\omega; G_i) = \frac{4\pi^2 e^2}{m^2 \omega^2 \hbar} \sum_{n \in G_i} \sum_{\substack{m=1 \\ m \notin G_i}}^{\infty} \int_{BZ} \frac{2d\mathbf{k}}{(2\pi)^3} p_{nm}^{\alpha}(\mathbf{k}) p_{mn}^{\beta}(\mathbf{k}) \delta(\omega_{mn}(\mathbf{k}) - \omega) \quad (\text{A4a})$$

$$\varepsilon''_{\alpha\beta}(\omega; G_i, G_j) = \frac{-4\pi^2 e^2}{m^2 \omega^2 \hbar} \sum_{n \in G_i} \sum_{m \in G_j} \int_{BZ} \frac{2d\mathbf{k}}{(2\pi)^3} p_{nm}^{\alpha}(\mathbf{k}) p_{mn}^{\beta}(\mathbf{k}) \delta(\omega_{mn}(\mathbf{k}) - \omega). \quad (\text{A4b})$$

The first sum of Eq. (A4a) has to be taken over the bands of group G_i while the second sum extends over all bands (unoccupied or not) except those of group G_i . In Eq. (A4b),

the two sums extend over the bands of group G_i and G_j . It is easy to show that $\varepsilon''_{\alpha\beta}(\omega; G_i)$ and $\varepsilon''_{\alpha\beta}(\omega; G_i, G_j)$ are related to the variances and covariances by the relations

$$\int_0^\infty \varepsilon''_{\alpha\beta}(\omega; G_i) d\omega = \frac{8\pi^2 e^2 n_i}{\hbar V_c} \langle r_\alpha r_\beta \rangle_c (G_i) \quad (\text{A5a})$$

$$\int_0^\infty \varepsilon''_{\alpha\beta}(\omega; G_i, G_j) d\omega = \frac{8\pi^2 e^2 n_i n_j}{\hbar V_c} \langle r_\alpha r_\beta \rangle_c (G_i, G_j). \quad (\text{A5b})$$

Thanks to these definitions, the physical meaning of the covariance becomes now obvious: If the total localization tensor was simply the sum of the variances $\langle r_\alpha r_\beta \rangle_c (G_i)$, the expression of the dielectric tensor (A1) would not only contain transitions between occupied and unoccupied states, but also transitions between occupied states themselves. It is by adding the covariances $\langle r_\alpha r_\beta \rangle_c (G_i, G_j)$ that one compensates the effect of these forbidden transitions in order to get a physically correct quantity.